

LNF-62/87
10. 10. 1962

G. Barbiellini, G. Bologna, G. Diambri, G. P. Murtas: MEASUREMENT OF THE POLARIZATION OF THE FRASCATI 1-GeV ELECTROSYNCHROTRON GAMMA-RAY BEAM FROM A DIAMOND CRYSTAL RADIATOR.

Nota interna: n° 162

Nota interna: n. 162
10 Ottobre 1962.

G. Barbiellini, G. Bologna, G. Diambri and G. P. Murtas:
MESUREMENT OF THE POLARIZATION OF THE FRASCATI 1-GEV
ELECTRONSYNCHROTRON γ -RAY BEAM FROM A DIAMOND CRY
STAL RADIATOR. -

In a previous letter⁽¹⁾ we showed experimental evidence for a line spectrum in the 1-GeV bremsstrahlung γ -ray beam obtained using a diamond radiator.

In this letter we give some results of the calculations and measurements concerning the polarization of a 150-MeV photon line. In high energy electron bremsstrahlung the radiated photons are emitted preferentially with a state of linear polarization parallel to the plane determined by the direction of the primary electrons and the recoil momentum of the nucleus.

In a crystal only those recoil momenta are allowed, which, in suitable units, are coincident with the reciprocal lattice vectors. Therefore the process is not symmetrical around the direction of the primary electron. It follows that the entire bremsstrahlung beam has a net polarization, with respect to a crystal plane.

The first calculation of this polarization was performed by Überall⁽²⁾; we have repeated it in order to take into account the discrete structure of the lattice planes. The importance of this structure has already been stated in other works^(1, 3).

A few numerical results of this calculation were given by us in reference 1. At the same time Überall also had recalculated the polarization, but his numerical data⁽⁴⁾ are not comparable with our experiment.

We define polarization of the entire γ -ray beam

$$(1) \quad P = \frac{I_H - I_V}{I_H + I_V}$$

where I_H and I_V represent the bremsstrahlung intensities for photons with polarization perpendicular and parallel, respectively, to the plane (\vec{p}_1, \vec{b}_1) , determined by the incident electron momentum \vec{p}_1 and a reciprocal lattice axis \vec{b}_1 .

The choice of the indices H and V is due to the fact that the (\vec{p}_1, \vec{b}_1) plane is held vertical. We obtained

$$(2) \quad I_H(\theta, x, E_1) - I_V(\theta, x, E_1) = 2(1-x) \psi_3^{**}(\theta, \delta)$$

$$(3) \quad \psi_3^{**}(\theta, \delta) = \frac{(2\pi)^2}{\Delta} 4 \int \sum_{\vec{g}} |F|^2 \frac{\exp(-Ag^2)}{(\beta^{-2} + g^2)^2} \frac{g_2^2 - g_3^2}{g_3^4 \theta^4}$$

where E_1 and k are the electron - and photon energy respectively, $x = k/E_1$, and θ is the angle between the vectors \vec{p}_1 and \vec{b}_1 .

The sum in (3) is extended over the reciprocal lattice vectors $\vec{g} = (0, g_2, g_3)$ which lie in the (\vec{b}_2, \vec{b}_3) plane; \vec{p}_1 lies in the (\vec{b}_1, \vec{b}_3) plane. The other quantities in formula (3) were already defined in ref. 1. In formula (1) one has

$$(4) \quad I_H(\theta, x, E_1) + I_V(\theta, x, E_1) = I(\theta, x, E_1)$$

I is the bremsstrahlung intensity, already defined in ref. 1.

The numerical values of formula (1) were calculated for diamond at room temperature, with the same input data as in ref. 1; the only difference is that now \vec{p}_1 is parallel to the plane of the axes $\vec{b}_1 = (110)$ and $\vec{b}_3 = (001)$. The reason is that in this situation the polarization is very large.

The continuous curve of fig. 1 represents formula (1) as a function of θ , and for $E_1 = 1$ GeV, $k = 150$ MeV.

The measurement of the polarization depends upon the fact that in electron pair production from linearly polarized photons the electrons are emitted preferentially in the plane of polarization (i. e., the plane determined by the direction of the incident photon \vec{k} and the polarization vector $\vec{\epsilon}$).

The experimental apparatus is about the same described in ref. 1. In the present experiment we chose a collimation of 1 mrad. The collimators were arranged in such a way to eliminate that part of the electron multiple traversals of the diamond radiator which spread out the γ -ray source in the horizontal direction. The source extension obtained in this way was ≈ 6 mm². The beam intensity after collimation was $\approx 10^{10}$ equivalent quanta/minute. The aluminum converter was 10^{-4} R. L. thick; in this way the mean square scattering angle of the electrons was much less than their most probable emission angle.

The principal change with respect to the old apparatus was made in the system of scintillation counters which detected symmetrical pairs. The present disposition is shown in fig. 2; the scintillators A_2 and A_3 , 10 cm in height, were placed in the e^- branch of the pair, while the scintillators A_1 and S_1 were placed in the e^+ branch. A_1 has the same height as A_2 and A_3 ; S_1 is only 0.5 cm in height. All the scintillators accepted an electron momentum spread $\Delta p/p = 8.5\%$.

By means of the triple coincidence $S_1 A_2 A_3$ we detected the symmetrical pairs in which one branch is emitted at any angle with respect to the incident photon and the other branch is emitted in the neighborhood of the spectrometer median plane MP, which is horizontal and contains S_1 .

On the other hand, by means of the triple coincidence A_1, A_2, A_3 we detected the symmetrical pairs with the two branches emitted at any angle.

The counting rate of $S_1 A_2 A_3$ depends on the position of the polarization plane; if this is horizontal, the counting rate is larger than if it is vertical. Olsen and Maximon⁽⁵⁾ calculated the pair production cross section from linearly polarized photons, integrated over the emission angles of one branch and differential in the emission angles of the other branch and, of course, in the electron energy.

In order to adjust this cross section to our experimental situation, we integrated it over the emission angle in the horizontal plane. We took into account also the electron multiple scattering in the converter as well as the finite size of the beam at the converter (its diameter was 1.3 cm), and the finite height of the scintillator S_1 . We obtained the asymmetry ratio

$$(5) \quad R = \frac{d\sigma_{\parallel} - d\sigma_{\perp}}{d\sigma_{\parallel} + d\sigma_{\perp}} = 10.1\% ,$$

for a photon energy $k = 150$ MeV; in formula (5) $d\sigma_{\parallel}$ and $d\sigma_{\perp}$ represent the pair production cross section in the given experimental situation, from photons polarized parallel and perpendicular to the spectrometer median plane respectively. R approaches zero when the converter thickness is more than 10^{-2} R. L. R is also decreased when the size of the γ -ray beam is increased. For this reason the 1-mrad angle of acceptance of the collimators was an upper limit.

In order to measure the polarization of the γ -ray beam we fixed the nominal energy of the photons at $k = 150$ MeV, by the proper choice of the spectrometer magnetic field and we measured the ratio of coincidence counts

$$(6) \quad \mathcal{P} = \frac{S_1 A_2 A_3}{A_1 A_2 A_3} ,$$

taking into account also delayed coincidences; background is negligible. We considered the coincidence $A_1A_2A_3$ only as a monitor in order to measure at constant number of photons. \mathcal{P} was measured for several values of θ , with \vec{p}_1 held parallel to the plane of the crystal axes $\vec{b}_1 = (110)$ and $\vec{b}_3 = (001)$, which is a vertical plane.

The relationship between formulas (6) and (1) is

$$(7) \quad \mathcal{P} = \mathcal{P}_0 (1 + RP)$$

from which we see that the constant \mathcal{P}_0 represents the values of \mathcal{P} for $P = 0$. Since for several reasons we could not yet measure the absolute value of the polarization, we assumed that the γ -ray beam was unpolarized at $\theta = \theta_0 = 5.8$ mrad, where the theoretical curve of Fig. 1 passes through the zero value. At this angle we measured \mathcal{P}_0 . Thus we made relative measurements, normalized at $\theta = \theta_0$.

Since the maximum value of P , on the basis of the theoretical results, is 50% and the value of R is 10%, the maximum relative difference between \mathcal{P} and \mathcal{P}_0 is 5%. Therefore we had to take particular care in measuring this small effect. In order to eliminate the bias introduced by the instability of the electronics, each measurement of \mathcal{P} was followed by a measurement of \mathcal{P}_0 ; we rejected those measurements in which the values of \mathcal{P}_0 differed more than the statistical error of $\approx 1\%$. We encountered another difficulty in the fact that the energies of the photons detected from the two triple coincidences $S_1A_2A_3$ and $A_1A_2A_3$ must be coincident within 1 MeV. In fact we see from Fig. 1b of ref. 1 the large rate with which the number of photons in the spectrum varies by changing the energy in the neighborhood of the first discontinuity; a change of 1 MeV in the photon energy will cause a change of some % in the number of counts and this is just of the order of the variation of \mathcal{P} .

If we could have rotated the crystal by 90° in its plane it would have been possible to measure an effect twice as large and besides would have been able to make an absolute measurement. However, due to experimental difficulties, this was not possible. We hope to overcome this difficulty shortly.

The experimental results are summarized in table 1. In the first column the value of the angle θ in milliradians is given; in the second column we give the weighted average

$$\left\langle \frac{\mathcal{P}}{\mathcal{P}_0} \right\rangle = \frac{\sum \frac{1}{\mu_i^2} \frac{\mathcal{P}^{(i)}}{\mathcal{P}_0^{(i)}}}{\sum \frac{1}{\mu_i^2}}$$

where μ_i is the error propagated in $\mathcal{P}^{(i)}/\mathcal{P}_0^{(i)}$ by the statistical errors of the counts $S_1A_2A_3$ and $A_1A_2A_3$.

TABLE I

Experimental results obtained in the measurement of the polarization			
θ (mrad)	$\langle \mathcal{P} / \mathcal{P}_0 \rangle$	$10^3 \mu_0$	P(%)
2.3	0.998	7.0	2^{+7}
2.9	1.002	9.6	6^{+10}
4.9	0.990	8.9	-6^{+9}
5.4	1.001	9.5	5^{+9}
5.8	1.000	4.5	4^{+4}
7.0	1.026	5.9	30^{+6}
7.4	1.049	4.8	52^{+5}
7.9	1.033	6.8	37^{+7}
9.0	1.029	7.1	33^{+7}
11.6	1.012	6.1	16^{+6}

In the third column we give the error of (8), i. e. ,

$$\mu_0 = \left[\sum (1/\mu_i^2) \right]^{-1/2} ,$$

multiplied by 10^3 .

In the fourth column we give the polarization P, calculated by means of the formula

$$(9) \quad \frac{\langle \mathcal{P} / \mathcal{P}_0 \rangle}{\langle \mathcal{P}_1 / \mathcal{P}_0 \rangle} = \frac{1 + RP}{1 + RP_1}$$

\mathcal{P}_1 being the value of \mathcal{P} obtained experimentally for $\theta = \theta_1 = 11.6$ mrad; $P_1 = 16.0\%$ is the theoretical value of the polarization at the same angle. The reason for which, in presenting the results, we prefer to re-normalize the data at $\theta = \theta_1$, is that at this angle the influence of the electron multiple scattering in the diamond is negligible.

In the same column, close to the value of the polarization its error is quoted. This is $\approx 10\mu_0$; i. e. in propagating the error by means of (9), we disregard the error of $\langle \mathcal{P}_1 / \mathcal{P}_0 \rangle$. This is because $\langle \mathcal{P}_1 / \mathcal{P}_0 \rangle$ is used only to normalize the theoretical and experimental behaviour of P.

The data of the fourth column are quoted also in fig. 1. The theoretical curve is not yet corrected for the electron multiple scattering in the diamond radiator. Nevertheless one can see how the variations of the polarization, as measured between an angle θ and the angle θ_1 , make a good fit with the theoretical curve, at least for $\theta > 6$ mrad; below this angle multiple scattering is important, so the experimental value do not agree well with the theoretical ones.

By inspection of fig. 1 we see that the polarizing device as well as the analyzing one, work satisfactory, because for a change of only $\Delta\theta = 1.6$ mrad, in the neighborhood of the discontinuity, we detected a change in polarization of

$$\Delta P = (48 \pm 7) \%$$

On the contrary, after substitution of the converter 10^{-4} R. L. thick with another one, 10^{-2} R. L. thick, the values of \mathcal{S} and \mathcal{P}_0 , relative to the preceding $\Delta\theta$, appeared coincident within the statistical error.

The big advantage in using a crystal instead of an amorphous radiator as a polarizer was indicated by Überall in his first work⁽²⁾. At this date we can say that the advantage is even greater than that expected at the time of the initial work.

We wish to thank Prof. J. DeWire for many valuable discussion and Dr. B. Antonini for the integration of the cross sections in formula (5).

-
- (1) - G. Barbiellini, G. Bologna, G. Diambrini and G. P. Murtas, Phys. Rev. Letters 8, 454 (1962); 9, 46 (1962) (Erratum).
 - (2) - H. Überall, Phys. Rev. 107, 223 (1957).
 - (3) - G. Barbiellini, G. Bologna, G. Diambrini and G. P. Murtas, Phys. Rev. Letters 8, 112 (1962).
 - (4) - H. Überall, Z. Naturforsch. 17, 332 (1962). Überall's numerical data are relative to only one reciprocal lattice row; thus they are different from ours, which were obtained by a sum over all reciprocal lattice points.
 - (5) - H. Olsen and L. C. Maximon, Phys. Rev. 114, 887 (1959)

Figure caption

Fig. 1 - Polarization of $k = 150$ -MeV photons in the entire bremsstrahlung beam of $E_1 = 1$ -GeV electrons, striking a diamond at room temperature. θ (in milliradians) is the angle between the momentum \vec{p}_1 of the incoming electron and the crystal axis $[110]$; \vec{p}_1 is parallel to the plane of the crystal axes $[110]$, $[001]$ (which is a vertical plane). $P = (I_H - I_V) / (I_H + I_V)$. The points represent the experimental results of table I. They are normalized to the theoretical curve at $\theta = 11.6$ mrad. The error is statistical.

Fig. 2 - Schetch of the analyzing device, \vec{k} is the direction of the incoming photon. $\vec{\epsilon}$ is the direction of the polarization vector. C is the aluminum converter. e^+ and e^- are the two branches of the symmetrical pair. \vec{B} is the direction of the magnetic field of the pair spectrometer. The height of the scintillators A_1 , A_2 , A_3 is 10 cm; that of S_1 is 0.5 cm. M. P. is the median plane of the pair spectrometer.

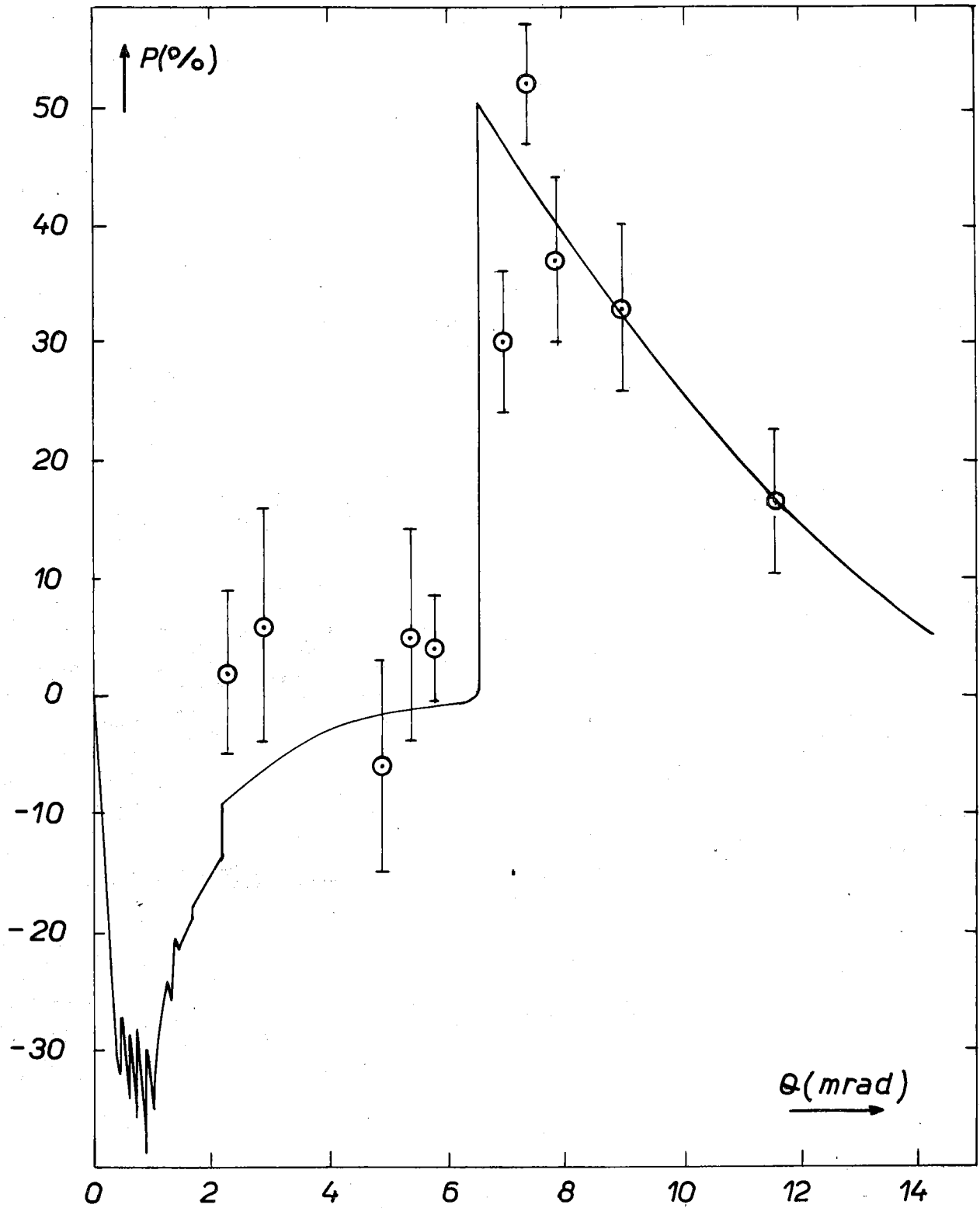


FIG. 1

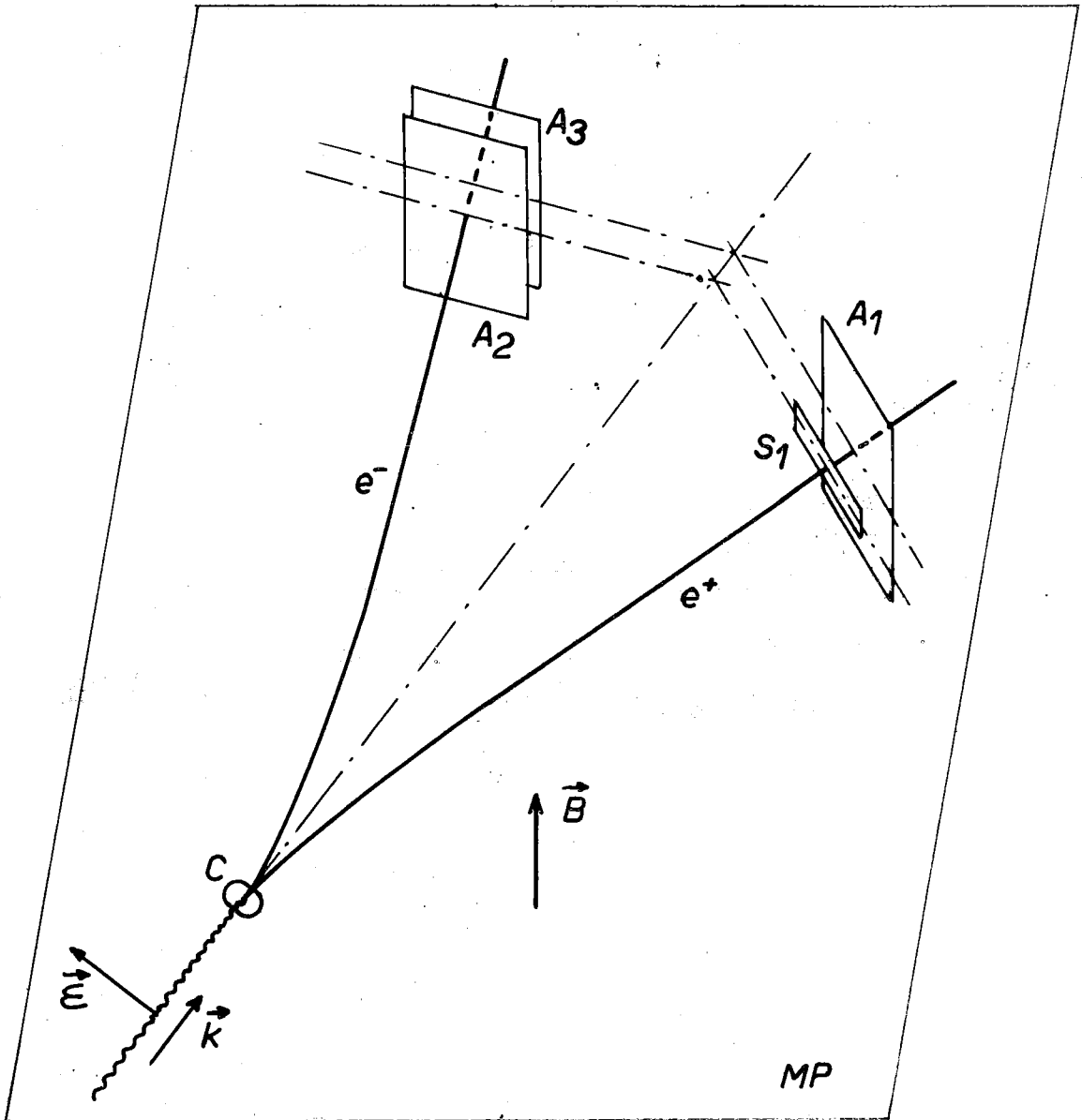


FIG. 2